Nanoscale potential barrier distributions and their effect on current transport in Ni/n type Si Schottky diode

M. Yeganeh†, N. Balkanian, and Sh. Rahmatallahpur

West North Research Complex, NSTRI, Bonab, Iran

Abstract: We have experimentally studied the Ni/n-Si nano Schottky barrier height (SBH) and potential difference between patches in the nano Schottky diodes (SD) using contact atomic force microscopy (C-AFM) in tapping mode and scanning tunneling microscopy (STM). Topology measurement of the surface with C-AFM showed that, a single Ni/n-Si SD consists of many patches with different sizes. These patches are sets of parallel diodes and electrically interacting contacts of 5 to 50 nm sizes and between these individual diodes, there exists an additional electric field. In real metal semiconductor contacts (MSC), patches with quite different configurations, various geometrical sizes and local work functions were randomly distributed on the surface of the metal. The direction and intensity of the additional electric field are distributed in homogenously along the contact metal surface. SBH controls the electronic transport across the MS interface and therefore, is of vital importance to the successful operation of semiconductor devices.

Key words: nano Schottky diode; additional electrical field; nanopatch; STM and C-AFM
DOI: 10.1088/1674-4926/36/12/124001 **EEACC:** 2520

1. Introduction

In recent years, in the real metal semiconductor contacts (MSC) there have been some investigations on the previously unknown natural phenomenon of an additional electric field (AEF). The AEF phenomenon has been an important object of experimental studies of Schottky diodes using scanning probe microscopy (SPM). The essence of the phenomenon of AEF is as follows[1−7].

According to the theoretical Schottky model, if the surface of a metalwith work function Φ_M is innear contact with the surface of an n-type semiconductor with work functions Φ_S, if $\Phi_M - \Phi_S \leqslant 0$, the contact has ohmic properties, and if $\Phi_M - \Phi_S \geqslant 0$, the contact has Schottky properties[1, 5−7]. In fact, in direct MSC with their free surface work function from 4 to 5 eV, the appearance of the contact potential difference between the contact surface and the adjacent free surfaces of the metal and semiconductor forms an AEF with an intensity of E_F around the side of the metal, which in micro- and nanocontact fully covers the contact region of the semiconductor. The historical development of MSC physics, the physical foundations of the AEF and the existing models for the formation of potential barriers have been described in References [1, 2, 7–13].

The most recent background of MSC of different sizes and shapes has been discussed in many journals in detail[6−8]. In some of them[14−17], the semiconductor-band-structure properties were measured directly at a subsurface interface with the C-AFM mode. Schottky barrier inhomogeneities in a Ni–n Si system were imaged with an energy resolution better than 0.1 eV. The average electrical behavior of trans rotational Ni layers used as contacts in diode structures on n-type Si was correlated to the local structure and conduction paths inside each patch by using C-AFM[10].

Even though the existence and effect of nanopatches in Schottky contacts have been investigated by different articles[11−15] and their electrical characteristics have been measured with different SPM modes, the study of AEF and its effect on electrical behavior of nano devices and Schottky type nano contacts is new and needs to be further analyzed.

In addition, in those references mechanisms of current transport, analytical formulas based on the theory of thermionic emission in the presence of AEF, and an effective method for determining electro physical and geometrical parameters of the contact's real and comparative analysis of the existing literary material in the interpretation of AEF have been described. Study of the phenomenon of AEF, the electronic processes associated in the real MSC, has caused a great deal of interest among scientists. In References [1–4] the detailed physical basis of the AEF phenomenon and the resulting electrical field and constructive-thermionic processes have been investigated with a comprehensive study in real AEF contact. The AEF phenomenon in the real MSC allows opening new research directions in the field of semiconductor physics and devices, solid state, thin films, surfaces, nanophysics, electronics, photo electronics, bioelectronics and nano electronics[5, 7, 15]. This phenomenon allows for a more deep and detailed interpretation of the processes occurring in actual contact structures of condensed matter. AEF is a phenomenon of the scientific basis for improving the quality and extending the functionality of semiconductor devices and circuits based on the nano structure's contacts. These structures constitute the basic elements of all kinds of instruments and modern electronics devices. The MSC converting light energy into electrical energy has already been developed, where the photocurrent-EMF far exceeds the dark current. Meanwhile, in the same transducer without the AEF, photovoltage exceeds the dark current about several times. In addition, the recently identified[16−20] new

† Corresponding author. Email: myeganeh@bnrc.ir
Received 22 April 2015, revised manuscript received 24 June 2015

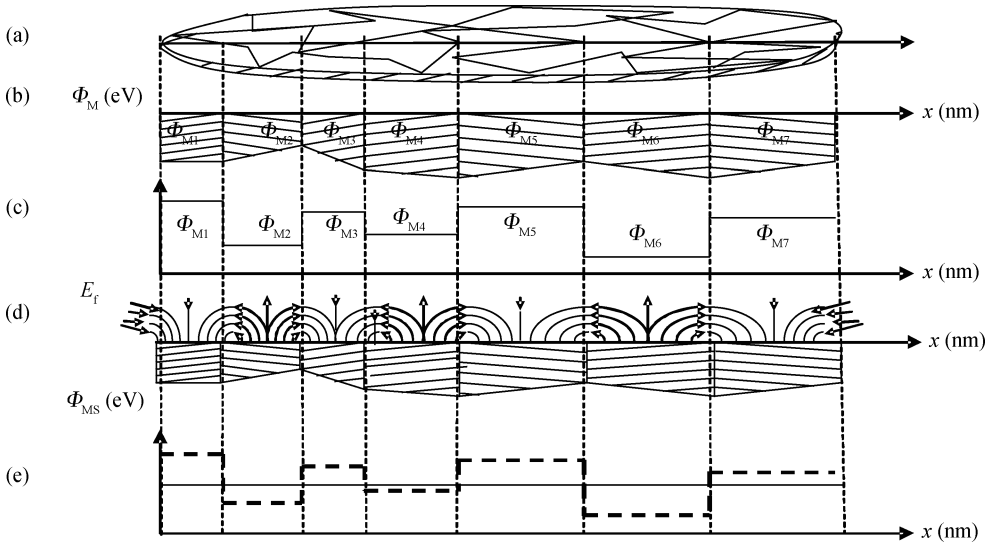

Figure 1. (a) Schematic diagrams of inhomogeneous surface (surfaces containing various micro and nano crystals. (b) Various local work functions. (c) Local surface work functions along ox axis. (d) Electric spot field E_f. (e) Average work functions in eV.

properties to the contact AEF, in which the reverse current is completely absent in the initial voltage and increases abruptly with further increase in voltage[4, 13, 20].

For studying the AEF phenomena, the development of SPM based probe techniques for the surface investigation provides a qualitatively new level of investigations of electro physical properties of the MSCs[21, 22].

In this work, considering the AEF in between nano patches and contacts free surfaces we investigate by the SPM method—the formation of nano layer Ni films on n-Si substrates, SB current transport mechanisms and electrical behaviors.

2. Theory

Theoretical and experimental values of the metal work function are different[1, 2, 13, 22]. In general for polycrystalline and single crystalline substances, the work function values are in the range of 2–6 eV. Moreover, polycrystalline substances, having various micro and nanocrystallographic orientations (known patches), possess different work function values. Typical diagrams of inhomogeneous metal surfaces have been given in Figure 1(a). For example on the surface along the ox axis, we consider seven patches with localized work functions Φ_{M1}, Φ_{M2}, Φ_{M3}, Φ_{M4}, Φ_{M5}, Φ_{M6}, and Φ_{M7} as shown in Figure 1(b). As summing that $\Phi_{M1} > \Phi_{M2} < \Phi_{M3} > \Phi_{M4} < \Phi_{M5} > \Phi_{M6} < \Phi_{M7}$, variations of local work functions along the ox axis are presented in Figure 1(c). It is supposed that the patches with different local surface work functions are in direct electric contact with surrounding patches, therefore, a potential difference between surfaces of patches, the so-called electrostatic spot field E_f, is formed as shown in Figure 1(d)[1, 3, 7].

The direction of the spot field is such that it decelerates electrons emitted by the areas possessing smaller work functions and accelerates the electrons from the areas with larger work functions. Consequently, the average work function Φ_{MS} remains constant along the ox axis (see the continuous line in Figure 1(e). In the presence of the spot fields, the work function Φ accomplished by an electron to remove from the Fermi level of the emitter and move to infinity is unequal to local work functions of the different parts of the surface.

In the absence of an external electric field, the average workfunction $\bar{\Phi}_M$ of the removal of an electron is identical for all parts of the surface and determined by

$$\bar{\Phi}_M = \frac{\int_S \Phi_M(s)\mathrm{d}S}{S}, \tag{1}$$

where S is the surface area of the emitter, $\Phi_M(s)$ is the LBH in the individual surface and $\bar{\Phi}_M$ is the work function, averaged over the total surface of the diode. The local work function in the spot field is positive for the section where $\Phi_M < \Phi_S$, and negative for the section where $\Phi_M > \Phi_S$. According to the thermionic emission theory, in the ideal SD, the potential barrier height Φ_{BO} is given by $\Phi_{BO} = \Phi_M - \chi$, where Φ_M is the metal work function and χ is the electronic affinity of the semiconductor. Φ_{BO} decreases under the action of the mirror image force with the value of the $\Delta\Phi_B$. The maximum barrier height is distance x_M from the surface of the metal (where x_M = 1–2 nm), and the I–V characteristic is expressedby[1]:

$$\begin{aligned} I &= SA^*T^2 \exp\left(-\frac{\Phi_B - \Delta\Phi_B}{kT}\right)\left(\exp\frac{qV}{kT} - 1\right) \\ &\approx SA^*T^2 \exp\left(-\frac{\Phi_B}{kT}\right)\exp\frac{qV}{nkT}, \end{aligned} \tag{2}$$

where

$$\Delta\Phi_B = q\left[\frac{q^3 N_D}{8\pi^2\varepsilon_{y/k}^3}\left(V_D \pm V - \frac{kT}{q}\right)\right]^{1/4}. \tag{3}$$

Here, S is the area of contact, A^* is the Richardson's constant, T is the absolute temperature, k is the Boltzmann's constant, q is the electron charge, V is the applied voltage, V_D is the diffusion potential, N_D is theconcentration of impurity, and ε_s is the dielectric permeability of the semiconductor.

With consideration of the AEF effect, nano Ni/n-Si SD I–V characteristics at the forward bias ($V > 0$) and under the condition of $qV \gg kT$ is expressed by[1]:

$$\begin{aligned} I_{\mathrm{F}} &= SA^{*}T^{2}\exp\left(-\frac{\Phi_{\mathrm{B}}}{kT}\right)\left[\exp\left(\frac{qV}{kT}\right)-1\right] \\ &= SA^{*}T^{2}\exp\left(-\frac{\Phi_{\mathrm{Bo}}+\beta_{\mathrm{f}}qV}{kT}\right)\exp\left(\frac{qV}{n_{\mathrm{r}}kT}\right) \\ &= I_{0}\left[\exp\frac{(1-\beta_{\mathrm{f}})qV}{kT}-\exp\left(-\frac{\beta_{\mathrm{f}}qV}{kT}\right)\right] \\ &= I_{0}\left[\exp\frac{qV}{n_{\mathrm{f}}kT}-\exp\frac{(1-n_{\mathrm{f}})qV}{n_{\mathrm{f}}kT}\right] \\ &\approx I_{\mathrm{o}}\exp\frac{qV}{n_{\mathrm{f}}kT}, \end{aligned} \tag{4}$$

$$I_{\mathrm{OF}} = SA^{*}T^{2}\exp\left(-\frac{\Phi_{\mathrm{BD}}}{kT}\right), \quad \beta_{\mathrm{f}} = \frac{n-1}{n}, \tag{5}$$

where Φ_{BD} is the operating potential barrier height, and β_{f} is the proportionality factor in forward bias.

Therefore, it is possible to draw a conclusion that the operating potential barrier on the contact surface of metal satisfiesthe equation $\Phi_{\mathrm{BO}} \leqslant \Phi_{\mathrm{BD}} - \beta_{\mathrm{r}}qV$. With consideration of the AEF effect, the I–V characteristics of nano SD at a reverse biasfor $V > V_{\mathrm{C}}$ are expressed by[6]:

$$\begin{aligned} I_{\mathrm{R}} &= SA^{*}T^{2}\exp\left(-\frac{\Phi_{\mathrm{BD}}-\beta_{\mathrm{r}}qV}{kT}\right)\left[\exp(\frac{q(V-V_{\mathrm{c}})}{kT})-1\right] \\ &= SA^{*}T^{2}\exp\left(-\frac{\Phi_{\mathrm{BD}}}{kT}\right)\left[-\frac{q(1-\beta_{\mathrm{r}})V-V_{\mathrm{C}}}{kT}\right] \\ &\quad\times\left(-\exp\frac{qV}{n_{r}kT}\right), \end{aligned} \tag{6}$$

where

$$I_{\mathrm{OR}} = SA^{*}T^{2}\exp\left(-\frac{\Phi_{\mathrm{BD}}}{kT}\right), \quad \beta_{\mathrm{r}} = \frac{1}{n_{\mathrm{r}}}. \tag{7}$$

In addition, at the voltage in an interval of $V \leqslant V_{\mathrm{C}}$, the current I_{R} is almost equal to zero.

To give the I–V characteristics of the nano diodes that consist of the real MSC, we use the STM mode of the SPM. In STM mode bias voltage was applied between a tip and the metal surface, so when the sample approaches to a few angstroms from the tip, tunneling current occurs, which indicates the proximity of the tip to the sample with very high accuracy. STM gives the true atomic resolution on some samples even at ambient conditions. STM can be applied to the study of small objects deposited on conductive substrates. LBH spectroscopy provides information about the spatial distribution of the microscopic work function of the surface, as described below. The tunneling current (I_{T}) in STM exponentially decays with the tip-sample distance (z) as:

$$I_{\mathrm{T}} \approx \exp(-2kz), \tag{8}$$

where z is the distant between the sample and the tip, and k is the spring decay constant given by:

$$k = (2m_{\mathrm{e}}\Phi/h^{2})^{1/2}, \tag{9}$$

where m_{e} is the effective electron mass, and h is the plank constant.

In the LBH imaging, we measure the sensitivity of the tunnel current to the tip-sample separation at each pixel of an STM image. The LBH obtained in this method is the so-called apparent barrier height Φ defined by[19]:

$$\Phi = 0.95(1/I_{\mathrm{T}})^{2}(\mathrm{d}I_{\mathrm{T}}/\mathrm{d}z)^{2}. \tag{10}$$

This value of Φ was compared to an average work function:

$$\Phi_{\mathrm{av}} = (\Phi_{\mathrm{s}} + \Phi_{\mathrm{t}})/2, \tag{11}$$

where Φ_{t} and Φ_{s} are the tip and sample work functions respectively.

In many cases, experimental V does not precisely agree with Φ_{av} but tends to be slightly smaller. Nevertheless, it is known that V is closely related to the local surface potential (local work functions) and is a good approximate measurement of the local surface potential. The LBH image was obtained by measuring point by point the logarithmic change in the tunneling current with respect to the change in the gap separation, that is, the slope of $\lg I$ versus z. In the LBH measurement, the tip-sample distance was modulated sinusoidally by an additional AC voltage applied to the feedback signal for the z-axis piezo device attached to the tip. The modulation period was chosen to be much shorter than the time constant of the feedback loop in the STM[21]. LBH spectroscopy can be used for providing information about the z-dependence of the microscopic work function of the surface. The next important use of $I(z)$ spectroscopy is concerned with testing the STM tip quality. In $I(z)$ spectroscopy, we measure the tunnel current versus the tip-sample separation at each pixel of an STM image. STM constants are $\Phi_{\mathrm{av}} = 1$ eV and $2k = 1.025\ \mathrm{A}^{-1}\mathrm{eV}^{-1}$. As mentioned above, we can use the STM mode of the SPM microscope, to directly measurethe work function of contact surfaces (patches)[28]. With C-AFM, we can also measure the electrical characters of every patch individually and study the AEF effect on the electrical behavior of nanopatches[19–22].

3. Experimental details

In most articles, the substrate being used to investigate the AEF and the current is a non-silicone substrate[1–3, 7]. The silicon substrate is very sensitive and it oxidizes immediately. However, because of the large use of silicon in the industry, we preferred to use silicon as a substrate. We also used nickel as a contact because of its ease of coating and its low prices. n-type Si with phosphor (P) impurity, crystal direction of (100) with a thickness of $575 \pm 15\ \mu$m and a resistivity of 4–11 Ω·cm was selected. One side of the sample surface was polished and for cleaning, the Radio Cooperation of America (RCA) method was applied. For making ohmic contact, we used high purity

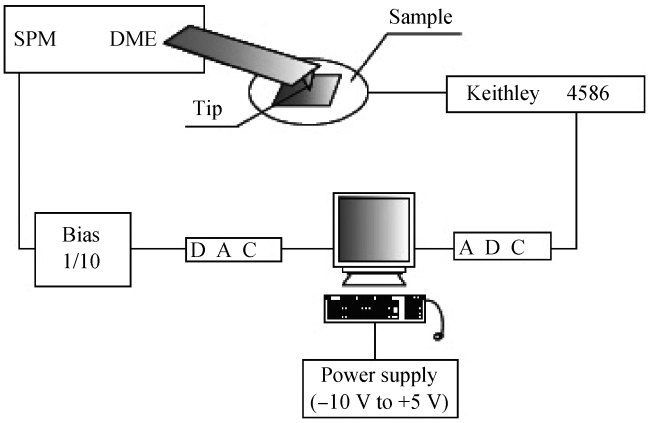

Figure 2. Experimental set up for surface measurements and device I–V characterizations.

(6N) Al with an electron beam gun coating system model EMS-160 made by the High Vacuum Technology Center (ACECR-Sharif University Branch-Iran). The sample was loaded in the chamber after cleaning. The deposition is under 5×10^{-5} Torr. After this stage, the samples were annealed in an oven with H_2 gas in 575 ℃ for 20 min. The 100 μm in diameter Schottky contacts were made by evaporating 0.12 μm of pure nickel on the polished side of the sample at a rate of 1.5 Å/s in a vacuum under 10^{-5} Torr. The substrate temperature was 25 ℃ and the coating system model was EMS-160. For studying the image profile, the phase difference in the cleaned surface of Si, the work function variation, nano patchesand I–V curves of the surface, we used the SPMDME dual C-26 system with AFM and STM modes. Figure 2 shows the experimental set up for surface measurements and device I–V characterizations.

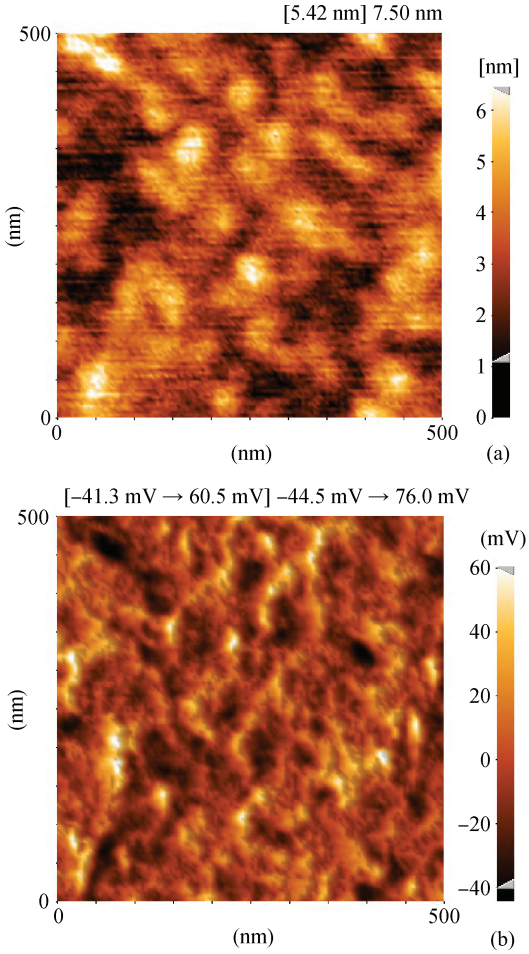

Figure 3. (Color online) (a) C-AFM topology image ofthe Si surface after the cleaning. (b) The surface potential distribution of the same surface.

4. Results and discussion

Although the surface condition is quite important in the discussion of Schottky barrier heights, the surface before depositing metal films is quite rough. The surface cleanness and surface atomistic structure should be checked carefully. For this, the proposed investigation of the topological and potential distribution of the surface with the C-AFM shows that, even with sufficient care in the preparation and cleaning of the Si surface, there is a potential difference of about 100 mV between different parts of the semiconductor surface. We perform the tapping mode for the morphology and C-AFM for surface potential. The changes in the surface work function were obtained by C-AFM in the LBH spectroscopy mode. This difference can be ignored in devices with dimensions in micrometers, but if the dimensions reduce to nanometers, this potential difference will reveal large electrical behavior differences. This is one source of different electrical behaviors of the device. Tiny polycrystalline areas and microscopic impurities on the surface are another important reason for this difference, which are not detectable with conventional equipment. In Figure 3(a), the morphology and the surface potential map of the Si surface after RCA cleaning are shown. The average surface-roughness is about 5.4 nm. Figure 3(b) shows the potential mapping (potential image). Potential changes are in the range of 100 mV. Investigation of the phase diagram shows that states and impurity levels of contamination were very low and are almost negligible; therefore, accurate cleaning removed the surface pollutions.

The nano metric localization of current transport in heterogeneous Schottky barriers was obtained by the combination of the electric field localization at the apex of a biased STM between the tip and Ni contact. The changes in the surface work function were obtained by STM in LBH spectroscopy mode. Figure 4(a) shows the morphology of the nickel layer surface coated on n-Si as the Schottky connection. Measurements of separate areas on the surface show that surface areas of nano-sized patches with approximate length of 5–50 nm have been formed. Patch distribution follows a Gaussian function with an average height of 13 nm. In Figure 4(b) the passing current image is given. Calculations of the surface work function changes along the line are shown in Figure 3(c). In addition, the work function changes of Figure 4(c) are in consistent with Figure 4(a).

In Figures 5(a) and 5(b) two images of the current through Ni contacts are reported with C-AFM. The potential difference was applied between the tip and the Si substrate to obtain these images. Figure 5(a) shows the current through the surface of the contact in a 0.5 V forward bias. For investigation of the effect of the potential difference of the patches on each other and

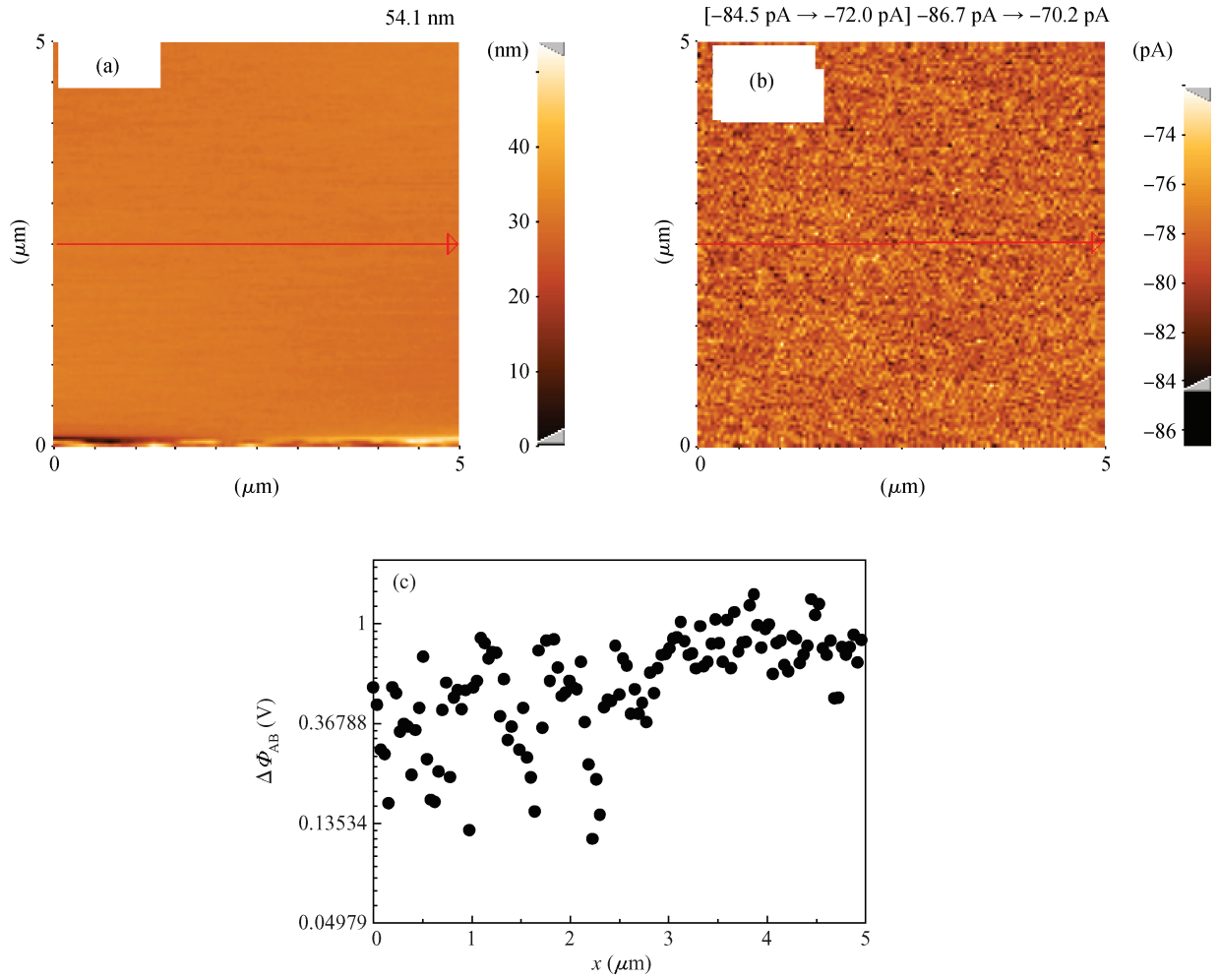

Figure 4. (Color online) (a) The morphology of nickel layer surface coated on n-Si. (b) Current passing from the surface. (c) Changes in the surface work function along the line.

thereby, the electrical behavior of nano-patches, part of Figure 5(a) is magnifiedand shown in Figure 5(b). Dark colors represent areas where more current passes through them.

From Figures 5(a) and 5(b), it was found that, independent from the patches' orientations, the central portion of the patch possesses a Schottky barrier lower than the rest of the structure. This was ascribed to the effect of AEF between the nano patches. The current transport through Schottky contacts was studied on nano scale patches by C-AFM. In Figure 6 different forward and reverse I–V characteristics of the nano scale patches are reported. These characteristics were measured with the scanning tunneling spectroscopy (STS) mode. For example, we report five different surface positions within a single macroscopic diode. The effective diameter of the diode considered to estimate the barrier height from forward I–V using thermionic emission theory is about 30 nm. The local current–voltage (I–V) measurements allow us to demonstrate the "laterally inhomogeneous" electrical behavior of the Ni–n Si contact, which was formed by a distribution of nano scale patches with different barrier heights. This behavior was explained in terms of the inhomogeneities of the Ni interface and of the electrically active AEF effect that presented in the Ni–nSi contact. The local Schottky barrier height at the interface between the single metal nanoparticle and the semiconductor was determined. Data of the Schottky barrier heights was measured on samples with different nano size distributions and the dependence of the barrier height on the nano size was demonstrated. In five examples, the forward bias of I–V characteristics as nano Ni/n-Si SD are well represented by forward lines in a wide interval of a current in half-logarithmic scale, and are similar to I–V characteristics of high-quality flat Ni/n-Si SD, where current transport is defined by the thermionic emission theory. According to Equation (4) the forward bias I–V characteristics of SD in the $kT < qV \leqslant \Phi_B$ interval is represented by a straight line in semi-logarithmic scale (Figure 6). The ideality factor n has constant value of 1.02–1.07. The reverse bias I–V characteristics SD are not saturated and with increasing of a reverse voltage up to the electric breakdown voltage, current slowly increases according to Equation (6). The linearity of I–V characteristics in half-logarithmic scale in forward voltage is up to 0.6 V. It means that series resistance of SD practically is negligible up to about 0.6 V. The series resistance of SD starts to influence at the voltage more than 0.6 V and therefore I–V characteristics of SD saturates. The increase in the ideality factor (n is caused by the increase in the potential barrier height of SD at βqV (i.e. $\Phi_B \approx \Phi_{BD} + \beta qV$).

The reverse bias of the I–V characteristics, as a single nano Ni/n-Si SD with a contact surface, essentially differ from

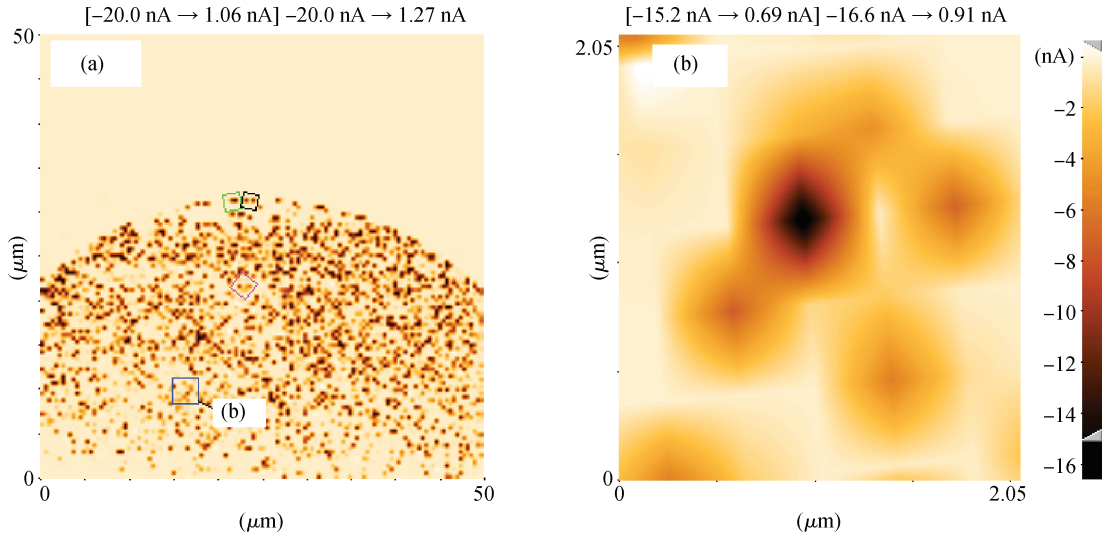

Figure 5. (Color online) (a) Image of current transport through contact patches in 0.5 V forward bias. (b) Magnified image of the amount of current transport in the selected areas with different colors in Figure 5(a).

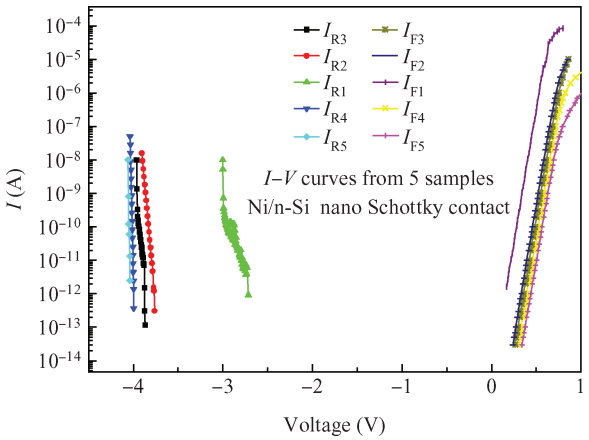

Figure 6. (Color online) I–V characteristics for five different nano diodes with STS mode of SPM in forward and reverse bias.

the reverse bias of I–V characteristics of a flat SD. With increasing the reverse voltage up to critical value V_C, the current is practically zero. In the lower voltage from V_C, with our measurement equipment (which can measure currents in the Femto Ampere range), the current could not be measured.There was no significant current and it can be assumed to be zero. By further increasing the voltage ($V > V_C$), the reverse current increases and jumps approximately in orders of 3–4. Further increasing the reverse voltage up to nearly $V_7 = 4.1$ V, the I–V characteristics are linear.

The series resistance of SD starts to influence at avoltage of more than 4.1 V. From the forward part of I–V curve I_F, n is from 1.07 to 1.046, Φ_{BD} from 0.945 to 0.852 eV and β from 0.11 to 0.08. As expected, the main effect of additional electric fields occurs in reverse bias. For all parts, reversecurrent is zero in the range of 2.7 to 4.1 V. Because of the identical manufacturing mechanism, the main reasons for the difference in voltage breakdown are the patch size distribution, the additional electric field influence and the intensity of the additional electric field obtained from different adjoining patches. From the endpart of the I–V curve, n is obtained from 1.17 to 1.076, Φ_{BD} from 0.965 to 0.812 eV and β from 0.11 to 0.08. As presented above, experimental forward and reverse I–V characteristics for nano SD and their corresponding analytical equations (4) and (6) satisfy the thermionic emission theory.

5. Conclusion

Measurement of the surface on thin metal film with C-AFM showed that Ni/n-Si SD consists of patches. These patches are sets of parallel connected and electrically cooperating nano-contacts of a size between 5 and 50 nm. Between these individual diodes are spot fields. It was shown that in real MSC, patches with quite different configurations, various geometrical sizes and local work functions were randomly distributed on the surface. The current transport and formations of potential barrier height in nano Ni/n-Si SD with a contact surface with awidth of 200–700 nm have been investigated. Features of current transport in reverse bias have specific features unlike the I–V characteristics of flat SD. The forward bias of the nano SD I–V characteristics are represented by straight lines in semi-logarithmic scale in a wide range, up to 0.7 V with a near ideality factor. In the beginning of the reverse voltage, the current was extremely low, by increasing the voltage the current jumped approximately by orders of 3–4 in the voltage range 2.5–4 V, then by increasing the voltage from 2.5 up to nearly 4.1 V, the current increased linearly.

References

[1] Mamedov R K. Features of the potential barrier and current flow in the narrow Schottky diodes. Superlattices and Microstructures, 2013, 60: 300

[2] Torkhov N A, Bozhkov V G. Fractal character of the distribution of surface potential irregularities in epitaxial n-GaAs (100). Semiconductors, 2009, 15743(5): 551

[3] Yeganeh M A, Rahmatallahpur S, Nozad A, et al. Effect of diode size and series resistance on barrier height and ideality factor in nearly ideal Au/n-type-GaAs micro Schottky contact diodes. Chin Phys B, 2010, 19(10): 10

[4] Monch W. Electronic structure of metal–semiconductor contacts. Phys Rev B, 1988, 37: 7129
[5] Tung R T. Recent advances in Schottky barrier concepts. Mater Sci Eng, 2001, 35: 1
[6] Schmitsdorf R F, Kampen T U, Monch W. Explanation of the linear correlation between barrier heights and ideality factors of real metal–semiconductor contacts by laterally nonuniform Schottky barriers. J Vac Sci Technol B, 1997, 15: 1221
[7] Yeganeh M, Rahmatallahpur S, Mamedov R K. Investigation of nano patches in Ni/n-Si micro Schottky diodes with new aspect. Materials Science in Semiconductor Processing, 2011, 14: 266
[8] Torkhov N A. Method to determine the interface's fractal dimensions of metal–semiconductor electric contacts from their static instrumental characteristics. Journal of Surface Investigation, X-ray, Synchrotron and Neutron Techniques, 2010, 4: 45
[9] Torkhova N A, Novikov V A. Fractal geometry of the surface potential in electrochemically deposited platinum and palladium films. Semiconductors, 2009, 43: 1071
[10] Mamedov R K, Yeganeh M A. Current transport and formation of energy structures in narrow Au/n-GaAs Schottky diodes. Microelectron Reliab, 2012, 52: 418
[11] Torkhov N A. Method to determine the interface's fractal dimensions of metal–semiconductor electric contacts from their static instrumental characteristics. Journal of Surface Investigation, X-ray, Synchrotron and Neutron Techniques, 2010, 4(1): 45
[12] Szkutnik P D, Piednoir A, Ronda A, et al. STM studies: spatial resolution limits to fit observations in nanotechnology. Appl Surf Sci, 2000, 164: 169
[13] Bell L D, Kaiser W J. Observation of interface band structure by ballistic-electron-emission microscopy. Phys Rev Lett, 1988, 61: 2368
[14] Giannazzo F, Roccaforte F, Raineri V, et al. Electrical properties of self-assembled nano-Schottky diodes. Europhys Lett, 2006, 74: 686
[15] Giannazzo F, Roccaforte F, Iucolano F, et al. Temperature dependence of electrical characteristics of Pt/GaN Schottky diode fabricated by UHV e-beam evaporation. J Vac Sci Technol B, 2009, 27: 789
[16] Hasegawa H, Sato T, Kasai S. Unpinning of Fermi level in nanometer-sized Schottky contacts on GaAs and InP. Appl Surf Sci, 2000, 166: 92
[17] Acar S, Karadeniz S, Tugluoglu N, et al. Gaussian distribution of inhomogeneous barrier height in Ag/p-Si (100) Schottky barrier diodes. Appl Surf Sci, 2004, 233: 373
[18] Pashaev I G. Electrophysical properties of Schottky diodes made on the basis of silicon with amorphous and polycrystalline metal alloy at low direct voltage. International Journal on Technical and Physical Problems of Engineering, 2012, 10(4): 41
[19] Song J Q, Ding T, Li J, et al. Scanning tunneling microscope study of nano sized metal–semiconductor contacts between $ErSi_2$ nano islands and Si (001) substrate. Surf Sci, 2010, 604: 361
[20] Vande Leemput L E C, van Kempen H. Scanning tunnelling microscopy. Rep Prog Phys, 2012, 55: 1165
[21] Alberti A, Giannazzo F. Nanoscale study of the current transport through transrotational NiSi/n-Si contacts by conductive atomic force microscopy. Appl Phys Lett, 2012, 101: 261906
[22] Ernst M, Hans J H, Roland B. Scanning probe microscopy: the lab on a tip. Springer, 2004: 210